

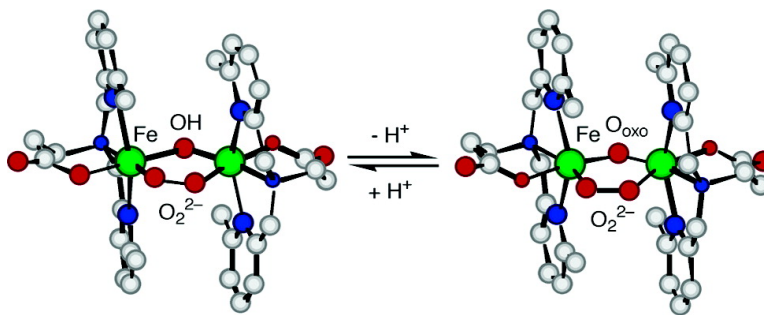
Communication

Structural and Spectroscopic Characterization of (η -Hydroxo or η -Oxo)(η -peroxy)diiron(III) Complexes: Models for Peroxo Intermediates of Non-Heme Diiron Proteins

Xi Zhang, Hideki Furutachi, Shuhei Fujinami, Shigenori Nagatomo, Yonezo Maeda, Yoshihito Watanabe, Teizo Kitagawa, and Masatatsu Suzuki

J. Am. Chem. Soc., **2005**, 127 (3), 826-827 • DOI: 10.1021/ja045594a • Publication Date (Web): 29 December 2004

Downloaded from <http://pubs.acs.org> on March 24, 2009



More About This Article

Additional resources and features associated with this article are available within the HTML version:

- Supporting Information
- Links to the 6 articles that cite this article, as of the time of this article download
- Access to high resolution figures
- Links to articles and content related to this article
- Copyright permission to reproduce figures and/or text from this article

[View the Full Text HTML](#)



ACS Publications
 High quality. High impact.

Structural and Spectroscopic Characterization of (μ -Hydroxo or μ -Oxo)(μ -peroxy)diiron(III) Complexes: Models for Peroxo Intermediates of Non-Heme Diiron Proteins

Xi Zhang,[†] Hideki Furutachi,^{*,†} Shuhei Fujinami,[†] Shigenori Nagatomo,[‡] Yonezo Maeda,[§] Yoshihito Watanabe,^{||} Teizo Kitagawa,[‡] and Masatatsu Suzuki^{*,†}

Department of Chemistry, Faculty of Science, Kanazawa University, Kakuma-machi, Kanazawa 920-1192, Japan, Center for Integrative Bioscience, Okazaki National Research Institutes, Myodaiji, Okazaki 444-8585, Japan, Department of Chemistry, Faculty of Science, Kyushu University, Higashi-ku, Fukuoka 812-8581, Japan, and Department of Chemistry, Graduate School of Science, Nagoya University, Chikusa-ku, Nagoya 464-8602, Japan

Received July 22, 2004; E-mail: suzuki@cacheibm.s.kanazawa-u.ac.jp

μ -1,2-Peroxydiiron(III) species have been spectroscopically identified as reaction intermediates for the dioxygen activating diiron proteins or some variants such as methane monooxygenase (MMO), ribonucleotide reductase (RNR), stearyl-acyl carrier protein Δ^9 -desaturase (Δ^9 D), and ferritin.^{1,2} Some of them are further activated to bis(μ -oxo)diiron(IV) or bis(μ -oxo)diiron(III,IV) species, which are responsible for oxidation of substrates. Diiron centers of those proteins have a common carboxylate-rich environment (four carboxylate and two N donors for MMO, RNR, and Δ^9 D). Various synthetic (peroxy)diiron(III) complexes including three structurally characterized complexes have been developed, and they provided a chemical basis for understanding of structural and various spectroscopic properties of the (peroxy)diiron complexes.^{3–6} To obtain further fundamental insights into structural and spectroscopic properties and reactivities of the (peroxy)diiron(III) species, further model (peroxy)diiron(III) complexes are needed, which have a biologically relevant ligand environment such as terminal carboxylate(s) and bridging hydroxide or oxide commonly found in diiron(III) forms.¹ Here, we report the first structurally characterized (μ -hydroxo)(μ -peroxy)diiron(III) complex [Fe₂(6Me₂-BPP)₂(OH)(O₂)]X (**2**; X: X = CF₃SO₃ (**2**·OTf), B(3-CIPh)₄ (**2**·B(3-CIPh)₄) and (μ -oxo)(μ -peroxy)diiron(III) complex [Fe₂(6Me₂-BPP)₂(O)(O₂)] (**3**) with a tripodal ligand (6Me₂-BPP)⁷ having a terminal carboxylate and the relationship among ligand environmental effects, spectroscopic properties, and reactivity.

Reaction of [Fe₂(6Me₂-BPP)₂(O)(OH)](OTf)·3.5H₂O (**1**)⁸ with ~100 equiv of H₂O₂ in methanol at –80 °C gave a blue complex **2**, which can be further converted to a purple complex **3** by addition of Et₃N. Crystal structure of **2**·B(3-CIPh)₄ showed that the complex has an Fe₂(μ -OH)(μ -1,2-O₂) core and each iron has a six-coordinate structure with N₃O₃ donors (Figure 1A). Two iron centers are inequivalent; the peroxy oxygen in the Fe1 site is trans to a tertiary amine nitrogen, while that in the Fe2 site is trans to a carboxylate oxygen. The structure of **3** is similar to **2**·B(3-CIPh)₄, but unfortunately, μ -oxo and μ -1,2-peroxy groups are disordered over two positions with 0.5 occupancy (Figure 1B). Detailed discussion about metric parameters of **3** may not be warranted, but comparison of the structural features with **2** is useful. The O1–O2 bond length of **2**·B(3-CIPh)₄ is 1.396(5) Å (cf. 1.41(1) Å for **3**), which is slightly shorter than those of the (peroxy)diiron(III) complexes (1.406(8)–1.426(6) Å).⁴ The Fe···Fe distance (3.396(1) Å) of **2** is comparable to those of the complexes with a bridging phenolate or alkoxide

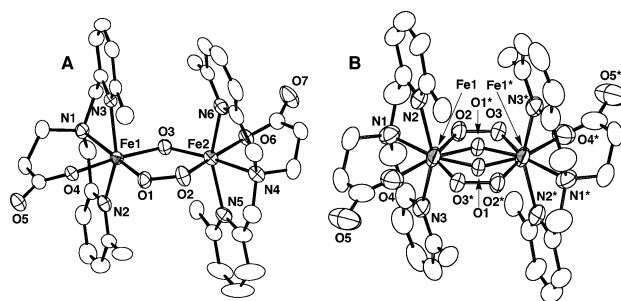


Figure 1. ORTEP views (50% probability) of **2**·B(3-CIPh)₄ (A) and **3** (B). Selected bond distances (Å) and angles (deg) for **2**·B(3-CIPh)₄: Fe1–O1, 1.867(4); Fe1–O3, 2.006(4); Fe1–O4, 1.986(4); Fe1–N1, 2.208(4); Fe1–N2, 2.232(5); Fe1–N3, 2.204(4); Fe2–O2, 1.887(4); Fe2–O3, 1.943(4); Fe2–O6, 1.999(4); Fe2–N4, 2.183(5); Fe2–N5, 2.193(5); Fe2–N6, 2.221(5); O1–O2, 1.396(5); Fe1···Fe2, 3.396(1); Fe1–O3–Fe2, 118.6(2); Fe1–O1–O2, 123.1(3); Fe2–O2–O1, 120.4(3); Fe1–O1–O2–Fe2, –14.5(4).

(3.327(2)–3.462(3) Å)^{4a,b} whereas longer than that of **3** (3.171(1) Å). Mössbauer spectra of **2**·B(3-CIPh)₄ and **3** at 80 K showed single quadrupole doublets with δ (ΔE_Q) = 0.50 (1.31) and 0.50 (1.46) mm/s, respectively. The ΔE_Q values are comparable to that of **1** (δ (ΔE_Q) = 0.44 (1.56) mm/s) but larger than that of [Fe₂(6Me₂-BPP)₂(OH)₂]²⁺ (**4**) (δ (ΔE_Q) = 0.42 (1.16) mm/s), suggesting that the peroxide also acts as a stronger π -donor and causes a larger electric field gradient around the Fe(III) centers as the oxo bridge.

It is noted that the bridging hydroxide and oxide significantly influence the spectroscopic properties. The electronic spectrum of **2**·OTf showed an intense peroxide (π_v^* orbital)-to-Fe(III) (d_π orbital) LMCT band⁵ at 644 nm (ϵ = 3000 M^{–1} cm^{–1}), whereas that of **3** showed a CT band at 577 nm (ϵ = 1500 M^{–1} cm^{–1}) (Figure 2). Such a significant blue shift and low intensity of the CT band of **3** can be partly ascribed to a stronger π -donation of the bridging oxide, which increases the d_π orbital energy of Fe(III) centers (diminishing the Lewis acidity of Fe(III) centers), increases the energy gap between d_π orbitals and π_v^* orbital of the peroxide, and decreases an overlap between them, leading to a blue shift and low intensity of the CT band.² The terminal carboxylate also influences the CT energy and reactivity. A closely related (μ -oxo)-(μ -peroxy)diiron(III) complex [Fe₂(6Me₃-tpa)₂(O)(O₂)]²⁺ (**5**) having N₄ donors exhibits a CT band at 648 nm (ϵ = 1200 M^{–1} cm^{–1}),^{6,9} which is red-shifted relative to that of **3**, indicating that the terminal carboxylate also functions as a stronger donor. In addition, **5** can be converted into a bis(μ -oxo)diiron(III,IV) species by O–O bond cleavage, which is accelerated by treatment of HClO₄. In contrast, no such conversion was detected for **3** and the reaction with HClO₄

[†] Kanazawa University.

[‡] Okazaki National Research Institutes.

[§] Kyushu University.

^{||} Nagoya University.

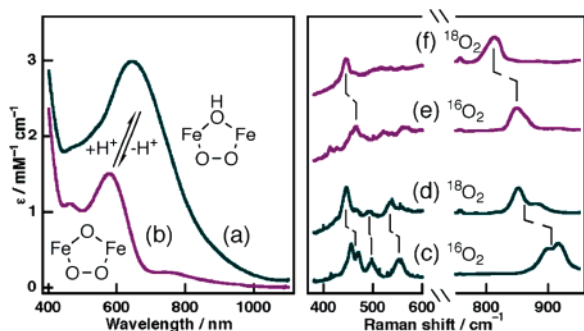


Figure 2. Electronic spectra of **2**·OTf (a) and **3** (b) in CH₃OH at $-80\text{ }^{\circ}\text{C}$ and resonance Raman spectra of **2** (prepared from H₂¹⁶O₂ (c) and H₂¹⁸O₂ (d)) and **3** (prepared from H₂¹⁶O₂ (e) and H₂¹⁸O₂ (f)) in CH₃OH at $-80\text{ }^{\circ}\text{C}$.

caused the conversion to **2**,¹⁰ suggesting an increase of basicity of the bridging oxide by stronger donation of the carboxylate in **3**.

The resonance Raman spectra of **2** and **3** (Figure 2c–f) showed several features which shifted downward by ¹⁸O-substitution. For complex **2**, we assigned two bands at 919 and 896 cm⁻¹ to the $\nu(\text{O}-\text{O})$ as a Fermi doublet (the intrinsic $\nu_{\text{O}-\text{O}}^0 = 908\text{ cm}^{-1}$; 881 and 850 cm⁻¹ for an ¹⁸O₂ sample, $\nu_{\text{O}-\text{O}}^0 = 861\text{ cm}^{-1}$).¹¹ The bands at 548 (¹⁸O₂: 536 cm⁻¹) and 498 (¹⁸O₂: 493 cm⁻¹) can be assigned to the $\nu_{\text{as}}(\text{Fe}-\text{O}-\text{O}) + \nu_{\text{as}}(\text{Fe}-\text{O}-\text{O})$ and $\nu_{\text{s}}(\text{Fe}-\text{O}-\text{O})$, respectively, based on normal coordinate analysis (NCA).¹² The analysis also indicated that the bands at 473 and 456 cm⁻¹ can be assigned to $\nu_{\text{s}}(\text{Fe}-\text{O}-\text{O})$ as a Fermi doublet ($\nu_{\text{Fe}-\text{O}}^0 = 460\text{ cm}^{-1}$; 447 cm⁻¹ for a ¹⁸O₂ sample). For complex **3**, a band at 847 cm⁻¹ (¹⁸O₂: 814 cm⁻¹) can be assigned to the $\nu(\text{O}-\text{O})$ and a band at 465 cm⁻¹ (¹⁸O₂: 446 cm⁻¹) to the $\nu_{\text{s}}(\text{Fe}-\text{O}-\text{O})$. The $\nu(\text{O}-\text{O})$ of **2** is similar to those of (peroxo)diiron(III) complexes (880–900 cm⁻¹),^{3,5} whereas it is significantly higher than that of **3** (847 cm⁻¹) and **5** (848 cm⁻¹).⁶ It has been shown that the $\nu(\text{O}-\text{O})$ and $\nu_{\text{s}}(\text{Fe}-\text{O}-\text{O})$ depend on the Fe–O–O angle; as the Fe–O–O angle becomes larger, the $\nu(\text{O}-\text{O})$ becomes higher and the $\nu_{\text{s}}(\text{Fe}-\text{O}-\text{O})$ becomes lower by mechanical coupling.⁵ This is also the case for **2** (Fe–O–O_{av} = 121.8°) and **3** (Fe–O–O = ~115°): the $\nu(\text{O}-\text{O})$ of **2** (908 cm⁻¹) is higher than that of **3** (847 cm⁻¹), and the $\nu_{\text{s}}(\text{Fe}-\text{O}-\text{O})$ of **2** (460 cm⁻¹) is lower than that of **3** (465 cm⁻¹). However, a large change in the $\nu(\text{O}-\text{O})$ ($\Delta = 61\text{ cm}^{-1}$) and a small change in the $\nu_{\text{s}}(\text{Fe}-\text{O}-\text{O})$ ($\Delta = 5\text{ cm}^{-1}$) between **2** and **3** also suggest the presence of some other contributions such as the bonding nature of the peroxide as observed for CT energies and intensities; the stronger donation of the peroxide in **2** increases the $\nu(\text{O}-\text{O})$ and $\nu_{\text{s}}(\text{Fe}-\text{O}-\text{O})$, leading to an increase of change in the $\nu(\text{O}-\text{O})$ and a decrease of change in the $\nu_{\text{s}}(\text{Fe}-\text{O}-\text{O})$ by an offset effect.¹³

It has been proposed that the changes in the $\nu(\text{O}-\text{O})$ and $\nu_{\text{s}}(\text{Fe}-\text{O}-\text{O})$ frequencies for RNR-W48F/D84E (868 and 457 cm⁻¹),^{2,14} $\Delta^9\text{D}$ (898 and 442 cm⁻¹),¹⁵ and ferritin (851 and 485 cm⁻¹)¹⁶ depend on the Fe–O–O angles. Very short Fe^{•••}Fe distances (~2.5 Å) have been reported for the peroxo-intermediates of ferritin¹⁷ and RNR-W48A/D84E.¹⁸ Such a short Fe^{•••}Fe distance requires a small Fe–O–O angle as observed for [Mn₂(L)₂(O)₂(O₂)²⁺ (Mn^{•••}Mn = 2.531(7) Å and Mn–O–O = 106.9°).¹⁹ However, for the relatively high $\nu(\text{O}-\text{O})$ frequency (868 cm⁻¹) of RNR-W48F/D84E, Solomon et al. pointed out that a short (2.5 Å) Fe^{•••}Fe distance reported for RNR-W48A/D84E which is proposed to be analogous to RNR-W48F/D84E is not supported from spectroscopic analyses for RNR-W48F/D84E.² A lower CT energy

of RNR-W48F/D84E (~700 nm) compared to those of the model complexes suggests the high Lewis acidity of Fe(III) centers in RNR-W48F/D84E relative to the model complexes except for [Fe₂{HB(3,5-*i*Pr₂pz)₃}(O₂)(PhCO₂)₂].^{2,5}

In summary, structures and spectroscopic properties of both (μ -hydroxo)(μ -peroxo) and (μ -oxo)(μ -peroxo)diiron(III) complexes provide fundamental chemical insights into the nature of (μ -1,2-peroxo)diiron(III) complexes, although further comprehensive structural and spectroscopic data of model complexes and proteins are needed.

Acknowledgment. Financial support of this research by the Ministry of Education, Science, and Culture Grant-in-Aid for Scientific Research to H. F., M. S., T. K., and Y. W. is gratefully acknowledged.

Supporting Information Available: Synthesis, X-ray crystallography, spectroscopic characterization, analyses of Fermi resonance, and NCA results. This material is available free of charge via the Internet at <http://pubs.acs.org>.

References

- (1) For example, see: (a) Merckx, M.; Kopp, D. A.; Sazinsky, M. H.; Blazyk, J. L.; Müller, J.; Lippard, S. J. *Angew. Chem., Int. Ed.* **2001**, *40*, 2782–2807. (b) Solomon, E. I.; Brunold, T. C.; Davis, M. I.; Kemsley, J. N.; Lee, S.-K.; Lehnert, N.; Neese, F.; Skulan, A. J.; Yang, Y.-S.; Zhou, J. *Chem. Rev.* **2000**, *100*, 235–349. (c) Wallar, B. J.; Lipscomb, J. D. *Chem. Rev.* **1996**, *96*, 2625–2657.
- (2) Skulan, A. J.; Brunold, T. C.; Baldwin, J.; Saleh, L.; Bollinger, J. M., Jr.; Solomon, E. I. *J. Am. Chem. Soc.* **2004**, *126*, 8842–8855.
- (3) For example, see: (a) Tshuva, E. Y.; Lippard, S. J. *Chem. Rev.* **2004**, *104*, 987–1012. (b) Tolman, W. B.; Que, L., Jr. *J. Chem. Soc., Dalton Trans.* **2002**, 653–660. (c) Bois, J. D.; Mizoguchi, T. J.; Lippard, S. J. *Coord. Chem. Rev.* **2000**, *200–202*, 443–485. (d) Girerd, J.-J.; Banse, F.; Simaan, A. J. *Struct. Bonding* **2000**, *97*, 145–177. (e) Que, L., Jr. *J. Chem. Soc., Dalton Trans.* **1997**, 3933–3940.
- (4) (a) Ookubo T.; Sugimoto, H.; Nagayama, T.; Masuda, H.; Sato, T.; Tanaka, K.; Maeda, Y.; Okawa, H.; Hayashi, Y.; Uehara, A.; Suzuki, M. *J. Am. Chem. Soc.* **1996**, *118*, 701–702. (b) Dong, Y.; Yan, S.; Young, V. G., Jr.; Que, L., Jr. *Angew. Chem., Int. Ed. Engl.* **1996**, *35*, 618–620. (c) Kim, K.; Lippard, S. J. *J. Am. Chem. Soc.* **1996**, *118*, 4914–4915.
- (5) Brunold, T. C.; Tamura, N.; Kitajima, N.; Moro-oka, Y.; Solomon, E. I. *J. Am. Chem. Soc.* **1998**, *120*, 5674–5690.
- (6) (a) MacMurdo, V. L.; Zheng, H.; Que, L., Jr. *Inorg. Chem.* **2000**, *39*, 2254–2255. (b) Dong, Y.; Zang, Y.; Shu, L.; Wilkinson, E. C.; Que, L., Jr.; Kauffmann, K.; Münck, E. *J. Am. Chem. Soc.* **1997**, *119*, 12683–12684.
- (7) Abbreviations used: 6Me₂-BPP = *N,N*-bis(6-methyl-2-pyridylmethyl)-3-aminopropionate; 6Me₃-tpa = tris(6-methyl-2-pyridylmethyl)amine; L = 1,4,7-trimethyl-1,4,7-triazacyclononane; HB(3,5-*i*Pr₂pz)₃ = hydrotris(3,5-isopropyl-1-pyrazolyl)borate.
- (8) Synthesis, X-ray crystallography, and spectroscopic characterization of the complexes are given in the Supporting Information.
- (9) Lower intensity of CT band of **5** relative to that of **3** suggests some other contributions together with the Lewis acidity of Fe(III) centers.
- (10) Complexes **2** and **3** can be reversibly converted by treatment of HClO₄ or Et₃N at $-80\text{ }^{\circ}\text{C}$ (see Figures S5 and S6).
- (11) Quantitative analyses of Fermi resonance are given in the Supporting Information.
- (12) NCA was performed by the Wilson GF matrix method with Urey–Bradley force field using ring models (Fe₂(μ -OH or O)(μ -O₂)) obtained by X-ray analyses. Reasonable fittings were obtained (see Supporting Information).
- (13) This is in line with larger force constants ($K(\text{O}-\text{O}) = 3.55$ and $K(\text{Fe}-\text{O}-\text{O}) = 2.18\text{ mdyne}/\text{\AA}$) for **2** relative to those of **3** ($K(\text{O}-\text{O}) = 3.25$ and $K(\text{Fe}-\text{O}-\text{O}) = 1.84\text{ mdyne}/\text{\AA}$).
- (14) Moënné-Loccoz, P.; Baldwin, J.; Ley, B. A.; Loehr, T. M.; Bollinger, J. M., Jr. *Biochemistry* **1998**, *37*, 14659–14663.
- (15) Broadwater, J. A.; Ai, J.; Loehr, T. M.; Sanders-Loehr, J.; Fox, B. G. *Biochemistry* **1998**, *37*, 14664–14671.
- (16) Moënné-Loccoz, P.; Krebs, C.; Herlihy, K.; Edmondson, D. E.; Theil, E. C.; Huynh, B. H.; Loehr, T. M. *Biochemistry* **1999**, *38*, 5290–5295.
- (17) Hwang, J.; Krebs, C.; Huynh, B. H.; Edmondson, D. E.; Theil, E. C.; Penner-Hahn, J. E. *Science* **2000**, *287*, 122–125.
- (18) Baldwin, J.; Krebs, C.; Saleh, L.; Stelling, M.; Huynh, B. H.; Bollinger, J. M., Jr.; Riggs-Gelasco, P. *Biochemistry* **2003**, *42*, 13269–13279.
- (19) Bossek, U.; Weyhermüller, T.; Wieghardt, K.; Nuber, B.; Weiss, J. *J. Am. Chem. Soc.* **1990**, *112*, 6387–6388.

JA045594A